Causal Decomposition Analysis
A Matlab Toolbox

Albert C. Yang, MD, PhD

Division of Interdisciplinary Medicine and Biotechnology
Beth Israel Deaconess Medical Center/Harvard Medical School, Boston, Massachusetts, USA

cyang1@bidmc.harvard.edu

V0.9, Jul 11, 2018

Contents

1. Introduction

Inference of causality in time series has been principally based on the prediction paradigm. Nonetheless, the predictive causality approach may underestimate the simultaneous and reciprocal nature of causal interactions observed in real world phenomena.

The **Causal Decomposition** method is developed not based on prediction, but based on the covariation of cause and effect: cause is that which put, the effect follows; and removed, the effect is removed.

Using empirical mode decomposition, we show that causal interaction is encoded in instantaneous phase dependency at a specific time scale, and this phase dependency is diminished when the causal-related intrinsic component is removed from the effect. Furthermore, we demonstrate the generic applicability of our method to both stochastic and deterministic systems, and show the consistency of causal decomposition method compared to existing methods, and finally uncover the key mode of causal interactions in both modelled and actual predator–prey systems.

This toolbox provides an array of MATLAB (Mathworks, Natick, MA) functions for quantifying the causal inference between a pair of time series, and for displaying the results in graphical form such as bar chart. The primary reference for the present toolbox is as follows:

> Yang AC, Peng CK, Huang, NE. Causal decomposition in the mutual causation system. *Nature Communication* (2018)

Which can be cited whenever this toolbox is used.

Comments, bug-fixes, and proposed enhancements are always welcome. The toolbox is free! And the toolbox is published under the GNU general public license (version 3, see www.gnu.org).

2. Installation

The installation of toolbox is fairly easy as shown in the following steps:

1. Unzip the compressed toolbox package in a directory (default directory name is: ~\causal_decomposition\)

2. In main menu of the MATLAB console, choose File -> Set Path, and a Set Path window will appear.

3. In Set Path window, select “Add with Subfolders…” and choose the main directory of Causal Decomposition toolbox (such as ~\causal_decomposition\).

4. Click “Save” to preserve the causal decomposition toolbox path whenever the MATLAB console is activated.

3. Causal decomposition analysis

3.1 Causal relationship based on instantaneous phase dependency

We define the cause–effect relationship between Time Series A and Time Series B according to the fundamental criterion of causal assessment proposed by Galilei (Galilei, 1960): cause is that which put, the effect follows; and removed, the effect is removed; thus, Variable A causes Variable B if the *instantaneous phase dependency* between A and B is diminished when the intrinsic component in B that is causally related to A is removed from B itself, but not vice versa.

$$Coh(A, B') < Coh(A, B) \sim Coh(A', B) \quad (1)$$

where *Coh* denotes the instantaneous phase dependency (i.e., coherence) between the intrinsic components of two time series, and the accent mark represents the time series where the intrinsic components relevant to cause effect dynamics were removed. The realisation of this definition requires two key treatments of the time series. First, the time series must be decomposed into intrinsic components to recover the cause–effect relationship at a specific time scale and instantaneous phase. Second, a phase coherence measurement is required to measure the instantaneous phase dependency between the intrinsic components decomposed from cause–effect time series.

3.2 Empirical mode decomposition

To achieve this, we decompose a time series into a finite number of IMFs by using the ensemble EMD (Huang et al., 1998; Z. Wu, Huang, Long, & Peng, 2007; Z. H. Wu & Huang, 2008) technique. Ensemble EMD is an adaptive decomposition method originated from EMD (i.e., the core of Hilbert-Huang Transform) for separating different modes of frequency and amplitude modulations in the time domain (Huang et al., 1998; Z. Wu et al., 2007).

Briefly, EMD is implemented through a sifting process to decompose the

original time-series data into a finite set of IMFs. The sifting process comprises the following steps: (1) connecting the local maxima or minima of a targeted signal to form the upper and lower envelopes by natural cubic spline lines; (2) extracting the first prototype IMF by estimating the difference between the targeted signal and the mean of the upper and lower envelopes; and (3) repeating these procedures to produce a set of IMFs that were represented by a certain frequency–amplitude modulation at a characteristic time scale. The decomposition process is completed when no more IMFs could be extracted, and the residual component is treated as the overall trend of the raw data. Although IMFs are empirically determined, they remain orthogonal to one another, and may therefore contain independent physical meanings (Lo, Novak, Peng, Liu, & Hu, 2009; Z. Wu et al., 2007).

The IMF decomposed from EMD enables us to use Hilbert transform to derive physically meaningful instantaneous phase and frequency (Geweke, 1982; Huang et al., 1998). For each IMF, they represent narrow-band amplitude and frequency-modulated signal *S(t)*, and can be expressed as

$$S(t) = A(t)cos\emptyset(t) \quad (2)$$

where instantaneous amplitude A and phase $\emptyset$ can be calculated by applying the Hilbert transform, defined as $S_H = \frac{1}{\pi}\int \frac{S(t')}{t-t'}dt'$; $A(t) = \sqrt{S^2(t) + S_H^2(t)}$; and $\emptyset(t) = \arctan(\frac{S_H(t)}{S(t)})$. The instantaneous frequency is then calculated as the derivative of the phase function $\omega(t) = d\emptyset(t)/dt$. Thus, the original signal X can be expressed as the summation of all IMFs and residual r,

$$X(t) = \sum_{j=1}^{k} A_j(t)exp\left(i\int \omega_j(t)dt\right) + r, \quad (3)$$

where k is the total number of IMFs, $A_j(t)$ is the instantaneous amplitude of each IMF; and $\omega_j(t)$ is the instantaneous frequency of each IMF. Previous literature have shown that IMFs derived with EMD can be used to delineate time dependency (Cummings et al., 2004) or phase dependency

(Cho, Min, Kim, & Lee, 2017; Hu, Lo, Peng, Liu, & Novak, 2012; Lo et al., 2009; Novak et al., 2004; Sweeney-Reed & Nasuto, 2007) in nonlinear and nonstationary data.

3.3 Ensemble EMD

The ensemble EMD (Z. Wu & Huang, 2004; Z. Wu et al., 2007; Z. H. Wu & Huang, 2008) is a noise-assisted data analysis method to further improve the separability of IMFs during the decomposition and defines the true IMF components $S_j(t)$ as the mean of an ensemble of trials, each consisting of the signal plus white noise of a finite amplitude.

$$S_j(t) = \lim_{N\to\infty} \frac{1}{N} \sum_{k=1}^{N} \{S_j(t) + r \times w_k(t)\} \quad (4)$$

where $w_k(t)$ is the added white noise, and *k* is the *k*th trial of the *j*th IMF in the noise-added signal. The magnitude of the added noise r is critical to determining the separability of the IMFs (i.e., r is a fraction of a standard deviation of the original signal). The number of trials in the ensemble *N* must be large so that the added noise in each trial is cancelled out in the ensemble mean of large trials (*N* = 1000 in this study). The purpose of the added noise in the ensemble EMD is to provide a uniform reference frame in the time–frequency space by projecting the decomposed IMFs onto comparable scales that are independent of the nature of the original signals. With the ensemble EMD method, the intrinsic oscillations of various time scales can be separated from nonlinear and nonstationary data with no *priori* criterion on the time-frequency characteristics of the signal. Hence, the use of ensemble EMD could complement the constraints of separability in Granger's paradigm (Yu, Li, Tang, & Wang, 2015) and potentially capture simultaneous causal relationships not accounted for by predictive causality methods.

3.4 Orthogonality and separability of IMFs

Because r is the only parameter involved in the causal decomposition analysis, the strategy of selecting r is to maximize the separability while

maintaining the orthogonality of the IMFs, thereby avoiding spurious causal detection resulting from poor separation of a given signal. We calculated the nonorthogonal leakage (Huang et al., 1998) and root-mean-square (RMS) of the pairwise correlations of the IMFs for each r with an increment of 0.05 in the uniform space between 0.05 and 1. A general guideline for selecting r in this study is to minimize the RMS of the pairwise correlations of the IMFs (ideally under 0.05) while maintaining the nonorthogonal leakage also under 0.05.

3.5 Phase coherence

Next, the Hilbert transform is applied to calculate the instantaneous phase of each IMF and to determine the *phase coherence* between the corresponding IMFs of two time series (Tass et al., 1998). For each corresponding pair of IMFs from the two time series, denoted as $S_{1j}(t)$ and $S_{2j}(t)$, and can be expressed as

$$S_{1j}(t) = A_{1j}(t)cos\emptyset_{1j}(t) \text{ and } S_{2j}(t) = A_{2j}(t)cos\emptyset_{2j}(t), \quad (5)$$

where A_{1j}, $\emptyset_{1j}$ can be calculated by applying the Hilbert transform, defined as $S_{1jH} = \frac{1}{\pi}\int \frac{S_{1j}(t')}{t-t'}dt'$, and $A_{1j}(t) = \sqrt{S_{1j}^2(t) + S_{1jH}^2(t)}$, and $\emptyset_{1j}(t) = \arctan(\frac{S_{1jH}(t)}{S_{1j}(t)})$; and similarly applied for S_{2jH}, A_{2j}, and $\emptyset_{2j}$. The instantaneous phase difference is simply expressed as $\Delta\emptyset_{12j}(t) = \emptyset_{2j}(t) - \emptyset_{1j}(t)$. If two signals are highly coherent, then the phase difference is constant; otherwise, it fluctuates considerably with time. Therefore, the instantaneous phase coherence *Coh* measurement can be defined as

$$Coh(S_{1j}, S_{2j}) = \frac{1}{T}\left|\int_0^T e^{i\Delta\emptyset_{12j}(t)}dt\right|. \quad (6)$$

Note that the integrand (i.e., $e^{i\Delta\emptyset_{12j}(t)}$) is a vector of unit length on the complex plane, pointing toward the direction which forms an angle of $\Delta\emptyset_{12j}(t)$ with the $+x$ axis. If the instantaneous phase difference varies

little over the entire signal, then the phase coherence is close to 1. If the instantaneous phase difference changes markedly over the time, then the coherence is close to 0, resulting from adding a set of vectors pointing in all possible directions. This phase coherence definition allows the instantaneous phase dependency to be calculated without being subjected to the effect of time lag between cause and effect (i.e., the time precedence principle), thus avoiding the constraints of time lag in predictive causality methods (Ding, Chen, & Bressler, 2006).

3.6 Causal decomposition between two time series

With the decomposition of the signals by ensemble EMD and measurement of the instantaneous phase coherence between the IMFs, the most critical step in the causal decomposition analysis is again based on Galilei's principle: the removal of an IMF followed by redecomposition of the time series (i.e., the decomposition and redecomposition procedure).

If the phase dynamic of an IMF in a target time series is influenced by the source time series, removing this IMF in the target time series (i.e., subtract an IMF from the original target time series) with redecomposition into a new set of IMFs results in the redistribution of phase dynamics into the emptied space of the corresponding IMF. Furthermore, because the causal-related IMF is removed, redistribution of the phase dynamics into the corresponding IMF would be exclusively from the intrinsic dynamics of the target time series, which is irrelevant to the dynamics of the source time series, thus reducing the instantaneous phase coherence between the paired IMFs of the source time series and redecomposed target time series. By contrast, this phenomenon does not occur when a corresponding IMF is removed from the source time series because the dynamics of that IMF are intrinsic to the source time series and removal of that IMF with redecomposition would still preserve the original phase dynamics from the other IMFs. Therefore, this decomposition and redecomposition procedure enables quantifying the differential causality between the corresponding IMFs of two time series.
Because each IMF represents a dynamic process operating at a distinct time scale, we treat the phase coherence between the paired IMFs as the

coordinates in a multidimensional space, and quantify the variance-weighted Euclidean distance between the phase coherence of the paired IMFs decomposed from the original signals as well as the paired original and redecomposed IMFs, which are expressed as follows:

$$D(S_{1j} \to S_{2j}) = \left\{\sum_{j=1}^{m} W_j\left[Coh(S_{1j}, S_{2j}) - Coh(S_{1j}, S'_{2j})\right]^2\right\}^{\frac{1}{2}}$$

$$D(S_{2j} \to S_{1j}) = \left\{\sum_{j=1}^{m} W_j\left[Coh(S_{1j}, S_{2j}) - Coh(S'_{1j}, S_{2j})\right]^2\right\}^{\frac{1}{2}}$$

$$W_j = (Var_{1j} \times Var_{2j}) / \sum_{j=1}^{m} (Var_{1j} \times Var_{2j}). \quad (7)$$

The range of D represents the level of absolute causal strength and is between 0 and 1. The relative causal strength between IMF S_{1j} and S_{2j} can be quantified as the relative ratio of absolute cause strength $D(S_{1j} \to S_{2j})$ and $D(S_{2j} \to S_{2j})$, expressed as follows:

$$C(S_{1j} \to S_{2j}) = D(S_{1j} \to S_{2j}) / [D(S_{1j} \to S_{2j}) + D(S_{2j} \to S_{1j})]$$

$$C(S_{2j} \to S_{1j}) = D(S_{2j} \to S_{1j}) / [D(S_{1j} \to S_{2j}) + D(S_{2j} \to S_{1j})]. \quad (8)$$

This decomposition and redecomposition procedure is repeated for each paired IMF to obtain the relative causal strengths at each time scale, where a ratio of 0.5 indicates either that there is no causal relationship or equal causal strength in the case of reciprocal causation, and a ratio toward 1 or 0 indicates a strong differential causal influence from one time series to another. To avoid a singularity when both $D(S_{1j} \to S_{2j})$ and $D(S_{2j} \to S_{1j})$ approach zero (i.e., no causal change in phase coherence with the redecomposition procedure), $D + 1$ is used to calculate the relative causal strength when both absolute causal strength D values are less than 0.05.

In summary, causal decomposition comprises the following three key steps:

(1) decomposition of a pair of time series *A* and *B* into two sets of IMFs (e.g., (IMFs *A* and IMFs *B*) and determining the instantaneous phase coherence between each paired IMFs.

(2) removing an IMF in a given time series (e.g., time series *A*), performing the redecomposition procedure to generate a new set of IMFs (IMF *A'*) and recalculating the instantaneous phase coherence between the paired original IMFs (IMFs *B*) and redecomposed IMFs (IMFs *A'*).

(3) determining the absolute and relative causal strength by estimating the deviation of phase coherence from the phase coherence of the original time series (IMFs *A* vs. IMFs *B*) to either of the redecomposed time series (e.g., IMFs *A'* vs. IMF *B*).

4. Applications

4.1 A quick tour

In the following quick tour, we will assess the causal inference of *Didinium* and *Paramecium* to investigate the mutual interactions between predator and prey.

This simple ecosystem demonstrates the periodic changes in the population of *Didinium* and *Paramecium.*

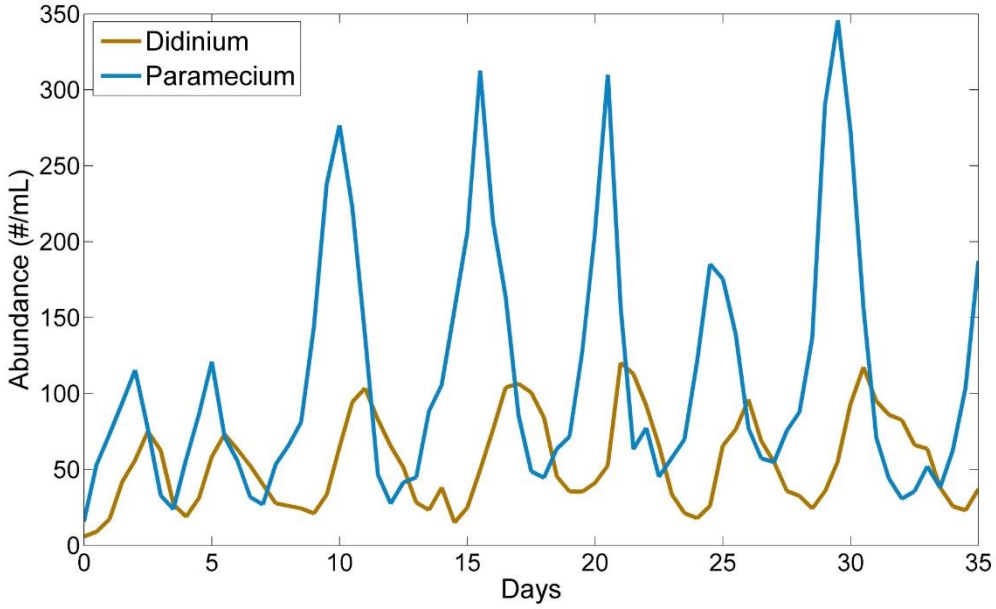

In this *in vitro* experiment, *Didinium* ingests the *Paramecium* to reduce the population of *Paramecium*. On the other hand, the population of *Didinium* is strictly dependent on the population of *Paramecium* as the source of food. Thus, the *Didinium* and *Paramecium* forms a mutual causation system.

The time series data is available publicly and can be accessed at [http://robjhyndman.com/tsdldata/data/veilleux.dat]. While we also include the data in this toolbox, an appropriate citation for this data is: Hyndman RJ. Time Series Data Library [http://robjhyndman.com/tsdldata/data/veilleux.dat] (2012)

1. First, we need to load the time series data into Matlab workspace.

```
load ecosystem_data.mat
```

The Matlab datafile contains the three sets of ecosystem data we presented in the *Nature Communication* paper, including time series of *Didinium* and *Paramecium*, hare and lynx, and wolf and moose data.

2. Second, we can visualize IMFs decomposed from a pair of time series using the example of *Didinium* (DIDI) and *Paramecium* (PARA). Note that the time series has been normalized by zero mean and one standard deviation. The purpose of the visualization is to examine the temporal relationship between the intrinsic components of the time series.

```
plot_pairedimfs(time_DIDIPARA,DIDI,PARA,0.35,1000,[]);
```

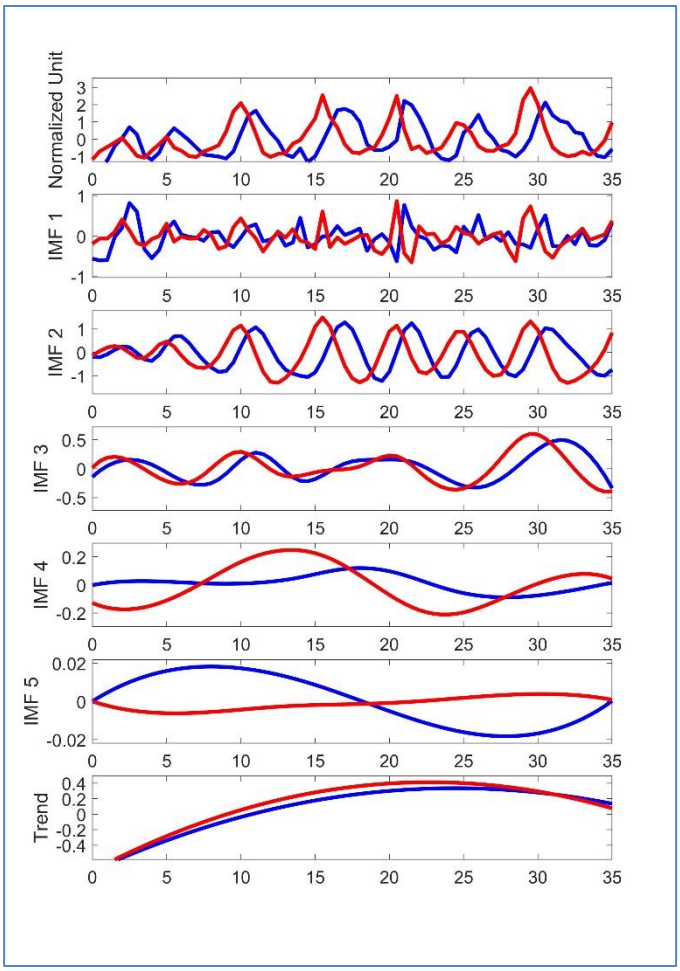

3. Third, we can calculate the causal matrix using causal decomposition analysis. Here we use the parameters of the noise level of 0.35 (the fraction of the standard deviation of the time series) and the number of ensemble of 1000 times. The number of ensemble affects the error (or degree of distortion by added noise) of IMFs. The degree of distortion can be reduced by a large number of trials and is estimated as noise level divided by the square root of the number of ensemble, which is equal to 0.011 in this case. The degree of distortion is suggested to be less than 0.05 in the ensemble EMD.

However, the key parameter here is the noise level, because the noise level determines the ability of ensemble EMD to separate the intrinsic components of a given time series. Too much noise will result in distorted signal even with a high number of ensemble trials. In contrast, a low noise level might result in the poor separation (e.g., mode mixing) of intrinsic component and biased causal assessment. The noise level can be determined using orthogonality and separability tests described in the section **3.4**.

```
causal_matrix = causal_decomposition(DIDI,PARA,0.35,1000)
```

```
causal_matrix =

    0.4977    0.5023    0.0234    0.0329
    0.5931    0.4069    0.3063    0.2102
    0.4966    0.5034    0.0140    0.0278
    0.5006    0.4994    0.0068    0.0044
    0.4999    0.5001    0.0001    0.0005
```

The output of causal_decomposition function contains a four by n matrix, where n is the number of IMFs decomposed from the data. The first column in the matrix indicates the relative causal strength from the first time series (DIDI) to the second time series (PARA) and vice versa in the second column. The third column indicates the absolute causal strength from DIDI time series to PARA time series, and vice versa in the fourth column.

The results indicate that causal interactions between DIDI and PARA have increased absolute causal strengths in IMFs 2 (second row), in which the absolute causal strength is higher from DIDI to PARA than that in opposite causal direction. As a result, the relative causal strength of IMF 2 indicates a higher causal influence from DIDI to PARA.

The discovery of causal influences in IMF 2 is interesting, because the IMF 2 can be visually identified as the key mode of oscillations in the DIDI and PARA time series (see the visualization of IMFs in page 14). The absolute casual strengths in other IMFs are approaching zero, indicating the absence of causal influences in those time scales, as also shown in the results of relative causal strengths to be 50/50, indicating no causal influence is observed.

5. Functions

plot_pairedimfs

Visualization and comparisons of intrinsic mode functions (IMFs)

Syntax

plot_pairedimfs(t,s1,s2,rnoise,nensemble,imfindex)

Input Arguments

t:

time vector

s1:

time series 1

s2:

time series 2

rnoise:

The level of noise used in ensemble empirical mode decomposition. The rnoise value represents the fraction of standard deviation of time series (e.g., 0.1).

nensemble:

The number of ensemble to average the results of noise-assisted empirical mode decomposition. The error of IMFs equals to rnoise / sqrt(nensemble)

imfindex:

selection of IMFs to be shown in the figures (default: []; for all IMFs)

Output Arguments

None

Examples

```
load ecosystem_data.mat
plot_pairedimfs(time_DIDIPARA,DIDI,PARA,0.35,1000,[]);
```

causal_decomposition

calculate the absolute and relative causal strengths

Syntax

causal_matrix = causal_decomposition(s1,s2,rnoise,nensemble)

Input Arguments

s1:

time series 1

s2:

time series 2

rnoise:

The level of noise used in ensemble empirical mode decomposition. The rnoise value represents the fraction of standard deviation of time series (e.g., 0.1).

nensemble:

The number of ensemble to average the results of noise-assisted empirical mode decomposition. The error of IMFs equals to rnoise / sqrt(nensemble)

Output Arguments

causal_matrix:

Output of causal strengths in a four by n matrix (n: number of IMFs)

The first column indicates relative causal strength from time series 1 to 2

The second column indicates relative causal strength from time series 2 to 1

The third column indicates absolute causal strength from time series 1 to 2

The fourth column indicates absolute causal strength from time series 2 to 1

Examples

```
load ecosystem_data.mat
causal_matrix = causal_decomposition(DIDI,PARA,0.35,1000)
```

6. References

Cho, D., Min, B., Kim, J., & Lee, B. (2017). EEG-Based Prediction of Epileptic Seizures Using Phase Synchronization Elicited from Noise-Assisted Multivariate Empirical Mode Decomposition. *IEEE Trans Neural Syst Rehabil Eng, 25*(8), 1309-1318. doi: 10.1109/TNSRE.2016.2618937

Cummings, D. A., Irizarry, R. A., Huang, N. E., Endy, T. P., Nisalak, A., Ungchusak, K., & Burke, D. S. (2004). Travelling waves in the occurrence of dengue haemorrhagic fever in Thailand. *Nature, 427*(6972), 344-347. doi: 10.1038/nature02225

Ding, M., Chen, Y., & Bressler, S. L. (2006). Granger Causality: Basic Theory and Application to Neuroscience. In B. Schelter, M. Winterhalder & J. Timmer (Eds.), *Handbook of Time Series Analysis: Recent Theoretical Developments and Applications*: Wiley-VCH.

Galilei, G. (1960). *On Motion and On Mechanics* (I. E. Drabkin & S. Drake, Trans.): The University of Wisconsin Press.

Geweke, J. (1982). Measurement of linear dependence and feedback between multiple time series. *J Am Stat Assoc, 77*, 304-324.

Hu, K., Lo, M. T., Peng, C. K., Liu, Y., & Novak, V. (2012). A nonlinear dynamic approach reveals a long-term stroke effect on cerebral blood flow regulation at multiple time scales. *PLoS Comput Biol, 8*(7), e1002601. doi: 10.1371/journal.pcbi.1002601

Huang, N. E., Shen, Z., Long, S. R., Wu, M. L. C., Shih, H. H., Zheng, Q. N., . . . Liu, H. H. (1998). The empirical mode decomposition and the Hilbert spectrum for nonlinear and non-stationary time series analysis. *Proceedings of the Royal Society of London Series A-Mathematical Physical and Engineering Sciences, 454*(1971), 903-995.

Lo, M. T., Novak, V., Peng, C. K., Liu, Y., & Hu, K. (2009). Nonlinear phase interaction between nonstationary signals: a comparison study of methods based on Hilbert-Huang and Fourier transforms. *Phys Rev E Stat Nonlin Soft Matter Phys, 79*(6 Pt 1), 061924. doi: 10.1103/PhysRevE.79.061924

Novak, V., Yang, A. C., Lepicovsky, L., Goldberger, A. L., Lipsitz, L. A., & Peng, C. K. (2004). Multimodal pressure-flow method to assess dynamics of cerebral autoregulation in stroke and hypertension. *Biomed Eng Online, 3*(1), 39.

Sweeney-Reed, C. M., & Nasuto, S. J. (2007). A novel approach to the detection of synchronisation in EEG based on empirical mode decomposition. *J Comput*

Neurosci, 23(1), 79-111. doi: 10.1007/s10827-007-0020-3

Tass, P., Rosenblum, M. G., Weule, J., Kurths, J., Pikovsky, A., Volkmann, J., . . . Freund, H. J. (1998). Detection of n:m Phase Locking from Noisy Data: Application to Magnetoencephalography. *Phys Rev Lett, 81*, 3291-3294.

Wu, Z., & Huang, N. E. (2004). A study of the characteristics of white noise using the empirical mode decomposition method. *Proc Roy Soc Lond A, 460*, 1597-1611.

Wu, Z., Huang, N. E., Long, S. R., & Peng, C. K. (2007). On the trend, detrending, and variability of nonlinear and nonstationary time series. *Proc Natl Acad Sci U S A, 104*(38), 14889-14894.

Wu, Z. H., & Huang, n. E. (2008). Ensemble empirical mode decomposition: a noise assisted data analysis method. *Advances in Adaptive Data Analysis, 1*(1), 1-41.

Yu, L., Li, J., Tang, L., & Wang, S. (2015). Linear and nonlinear Granger causality investigation between carbon market and crude oil market: A multi-scale approach. *Energy Economics, 51*, 300-311.